Structural and magnetic properties of bcc Co films on Pt(001) studied by magnetic resonant surface x-ray diffraction, STM, and magneto-optical Kerr effect

S. M. Valvidares,[1,*] T. Schroeder,[1] O. Robach,[1] C. Quirós,[2] T.-L. Lee,[1] and S. Ferrer[1]
[1]*European Synchrotron Radiation Facility, BP 220, 38043 Grenoble cedex. France*
[2]*Departamento de Física, Facultad de Ciencias, Avda. Calvo Sotelo s/n, 33007 Oviedo, Spain*
(Received 25 May 2004; revised manuscript received 3 September 2004; published 14 December 2004)

The structure of Co epitaxial films deposited on Pt(001) has been investigated with scanning tunnelling microscopy and surface x-ray diffraction. The Co films grow in a layer-by-layer mode up to the highest examined thickness (~30 Å). Their crystalline structure is a tetragonal distortion of the bcc structure in pseudomorphic epitaxy with the substrate. It consists of a −1.8% in-plane compressive strain and 5.1% out-of-plane tensile strain. A similar pseudomorphic structure is also observed in Pt/Co/Pt(001) trilayers. The magnetic properties of the films have been investigated by transverse magneto-optical Kerr effect and magnetic-resonant surface x-ray diffraction. The films exhibit in-plane magnetic anisotropy easy axes within the thickness range of 5–30 Å. The magnetization curves of Co and interfacial Pt are similar, indicating ferromagnetic coupling.

DOI: 10.1103/PhysRevB.70.224413 PACS number(s): 75.70.Cn, 75.70.−i, 68.37.Ef, 75.70.Ak

I. INTRODUCTION

Artificially layered and low dimensionality magnetic systems are a field where a large research effort has been done, particularly due to their interest for information storage technology applications. The field is also very attractive for the potential use of these type of systems as magneto-electronic devices in future technology.[1–5] In particular, because of the occurrence of out-of-plane magnetic anisotropy,[8,9] systems like Co/Pd and Co/Pt,[6] Co/Au,[7] or some related alloys have been found to well suit the requirements of perpendicular magneto-optical recording media, which is interesting in view of achieving large storage densities. It is of practical importance that (i) the preparation of these systems in the form of multilayers solves the problem of obtaining magnetic films with a large enough perpendicular magnetic signal, as for thickness over about 1–2 nm there is a transition from perpendicular to in-plane magnetic anisotropy easy directions (the so-called spin reorientation transition); (ii) films with perpendicular anisotropy can be prepared by low cost production techniques like sputtering; (iii) the (111) orientation is the one that most naturally grow due to its lower free surface energy compared to other orientations, but also other orientations like the (001) can be obtained depending on preparation conditions and substrate selection.[6,10]

Complementary studies for different surface orientations or substrates, including systems with in-plane magnetic anisotropy as is the case of Co/Pt(001), are important to get a deeper insight into the different contributions to the magnetic anisotropy. These include interface effects related to roughness, intermixing and electronic coupling between the substrate and the film, strain effects due to the lattice misfit and magnetocrystalline contributions associated with the crystal structure of the film.[10,11]

In this work, we report structural and magnetic results of a growth study of Co ultrathin films on a Pt(001) single crystal.

Our results are discussed in connection with previous works on (001)-oriented Co/Pt multilayers[12–18] and Co films on a Pt(001) single crystal.[19–22] Due to the similarity between the Pt and Pd lattices, which differ by less than 1%, we also compare our results with those of Co/Pd(001).[23–26]

This paper is organized as the following. In Sec. II we deal with the experimental details. In Sec. III the growth and structural properties are presented. Section IV is dedicated to the magnetic properties. A final discussion and some concluding remarks are given in Sec. V.

II. EXPERIMENTAL DETAILS

The growth of cobalt epitaxial films on top of a reconstructed Pt(001) single crystal surface has been studied *in-situ* by surface x-ray diffraction (SXRD), transverse magneto-optical Kerr effect (TMOKE) and scanning tunneling microscopy (STM) techniques. X-ray and magneto-optical studies have been carried out at the Surface Diffraction Beamline ID3 of the ESRF,[27] and STM studies have been performed using a commercially available set-up working at room temperature in the constant current mode. The same Pt single crystal has been used in all the measurements. For SXRD studies, the Pt crystal lattice was spanned with the tetragonal basis $A_1 = A_2 = 2.774$ Å, and $A_3 = 3.923$ Å. In this way, the reciprocal space axes H and K are in the surface plane and L is along the surface normal. (HKL) values are expressed in Pt reciprocal lattice units (r.l.u). Two x-ray wavelengths were used: $\lambda = 1.075$ Å, corresponding to the Pt L_{III} absorption edge energy (11.564 keV), was utilized for the resonant diffraction experiments to probe the Pt magnetism,[28] and $\lambda = 0.726$ Å for the crystallographical studies since it allows us to access larger values in reciprocal space. Magnetic measurements were performed by applying a magnetic field created by an electromagnet with pole pieces entering the UHV chamber and allowing a maximum field of 1400 Oe at the sample. The magnetic field was always applied parallel to the surface, which corresponds to the vertical direction, i.e., transverse to the polarization of

the incoming x-ray beam. Further details of the methodology for magnetic diffraction measurements are given in previous work.[28,45,50] The magnetic diffraction signals are given in terms of the asymmetry ratio, R, defined as $R(H,K,L)=(I_{\uparrow}-I_{\downarrow})/(I_{\uparrow}+I_{\downarrow})$, where $I_{\uparrow}$ and $I_{\downarrow}$ stand for the diffracted intensities at (H,K,L) while switching the applied magnetic field. TMOKE measurements were carried out using a set-up based on a photoelastic modulator installed on the vacuum chamber. Resonant-magnetic SXRD and TMOKE measurements could be performed simultaneously in order to investigate the in-plane transverse component of the induced magnetization of the Pt atoms at the interface and of the magnetization of the Co layer, respectively. Each of the magnetization cycles was obtained by averaging successive data during about 15 minutes. Co and Pt layers were deposited using water-cooled electron bombardment evaporators. The evaporation rates were in the range of 0.05–0.20 ML/min for Co and ~0.01–0.02 ML/min for Pt (here ML stands for a monolayer and corresponds to 1.3×10^{15} Pt atoms/cm^2 or 1.6×10^{15} Co atoms/cm^2). During the evaporation and the study of the films, the pressure in the UHV chamber was in the 10^{-10} mbar range.

A clean reconstructed Pt(001) surface was obtained after several cycles of Ar^+ ion sputtering and short annealing treatments to 1000–1200 °C. Oxygen treatments consisting in exposures at 2×10^{-7}mbar for a few minutes at a temperature of 700 °C were also performed to remove residual surface carbon contamination. It was observed that when the surface reconstruction was partially lifted off because of the adsorption of residual gas, it could be recovered by a short anneal to temperatures between 150 and 400 °C and preserved for many hours.

III. GROWTH AND STRUCTURAL PROPERTIES

A. Clean reconstructed surface

Platinum (001)-*hex* was the first clean metal surface reconstruction to be reported in the surface science literature by Hagstrom *et al.*[29] in 1965 and over the last forty years it has been the object of extensive characterization by LEED, STM, and diffraction techniques.[30–34] Figure 1 is a high resolution STM image showing the characteristic features of the Pt(001)-hex surface reconstruction. The main feature of the hex layer are the characteristic rows of atoms running vertically in the figure. The misfit between the close-packed directions in the substrate and the reconstructed layer leads to a height modulation: along the rows (vertical direction in the figure) the corrugation is very small, ≤0.05 Å, whereas across the rows (horizontal direction) it is much larger, typically 0.15–0.30 Å. The inset in Fig. 1 shows that a quasi-hexagonal symmetry of the nearest neighbor coordination sphere exists in the reconstructed layer. The reconstructed surface unit cell depicted in the figure, is usually described in the Wood notation by $\begin{pmatrix} N & 1 \\ -1 & 5 \end{pmatrix}$, where N is found to vary between 12 and 14 depending on the preparation details.[30,31,33,34] *Ab initio* studies identified the tensile excess stress of the unreconstructed (1×1) surface as the driving mechanism for the reconstruction.[35] The reconstructed quasi-hexagonal surface layer contains 20% to 25% more Pt atoms than the square (1×1) surface plane and is energetically favored over the (1×1) phase by about 0.1 eV/atom.[36] As the CO adsorption energy on the Pt(001)-(1×1) surface is by about 0.2 eV/atom higher than on the Pt(001)-hex layer, residual amounts of CO in the UHV chamber lift the reconstruction.[36–38] Here, we performed a time-resolved STM study on the surface restructuring during the decay of the Pt(001)-hex layer towards the (1×1) surface phase ($P_{CO}=2-5\times10^{-11}$ mbar). Apart from the intrinsic interest of the process, this preliminary study is helpful for posterior discussion of the growth of the Co layer as, identically, the deposition of a Co monolayer also removes the surface reconstruction. It shows that the excess of Pt atoms of the reconstructed layer may be expected to be present at the surface in the form of small clusters. Implications for the case of a Co layer growth will be discussed in Sec. III B.

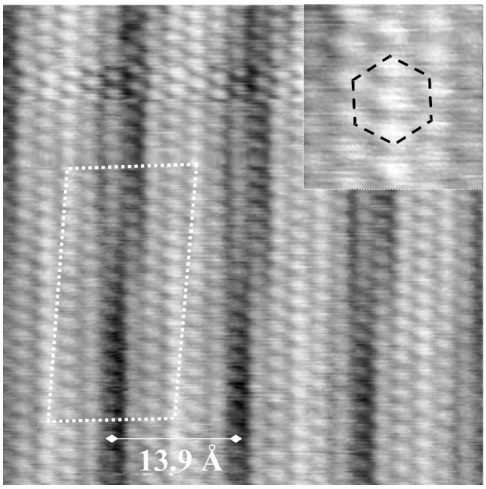

FIG. 1. STM image of the clean Pt(001)-hex reconstructed surface showing in detail the resulting arrangement in rows. The approximated surface unit cell is indicated. The close-to hexagonal local symmetry is manifest in the inset ($V_{gap}=0.002$ V; $I=30$ nA).

Figure 2(a) shows an overview scan. The Pt(001)-hex layer is clearly visible in the form of the characteristic line structure in the middle of the image but already lifted in the left and the right parts of the scan. The excess Pt atoms of the Pt(001)-hex layer remain on the unreconstructed (1×1) surface in the form of many small Pt islands with an average diameter of about 2–3 nm and monatomic step height. This condensation of the excess Pt atoms in little islands is well known and it was shown that the average Pt island size results from an interplay between surface mobility and the pair-wise interaction energy between adatoms on nearest-neighbor sites.[39] Nevertheless, the STM image sequence show that the excess Pt atoms form first very long Pt islands [marked by tilted arrows in Fig. 2(a)] when the decay of the reconstruction happens within a hex layer domain. This very different island morphology most likely results from an anisotropic effective diffusion barrier set up by the surrounding reconstructed hex layer. In this way, excess Pt atoms squeezed out of the hex surface are absorbed by the growing island before further critical nuclei for the growth of new islands are formed.[40] As the phase transition $hex\rightarrow(1\times1)$

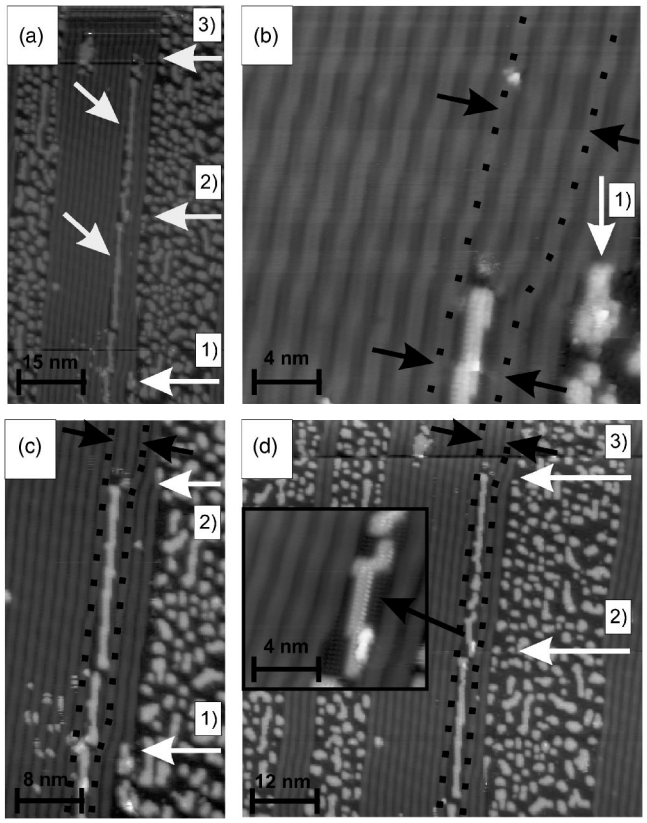

FIG. 2. Sequence of STM images showing details of the decay process of the surface reconstruction due to adsorption of residual gas (see the text). (V_{gap}=−0.01−0.02 V, I=30 nA).

was found to nucleate at heterogeneously originated surface defects,[36] the decay of the reconstruction within a hex domain points to the presence of a linear defect. An analogous case of nucleation on dislocation lines producing elongated dendritic islands was reported in Co/Pt(111).[41]

The development of the very long Pt island structure present in the overview scan of Fig. 2(a) can be followed in three different growth stages indicated by the horizontal arrows (1) to (3). The images in the sequence were taken about 8 h after the surface preparation and with time intervals between them of about 80 min (note that the time scale of the surface reconstruction decay was large enough to perform studies of Co films on top of a clean reconstructed surface). The starting point of our study is the growth stage (1) in Fig. 2(b) [the vertical arrow 1 marks the same island as in Fig. 2(a) to guide the reader]. The reconstruction is still intact above the Pt island within the hex layer but, as indicated by the dotted lines, a curvature of the neighboring reconstruction rows is observed. Pairs of black arrows indicate the distance between the dotted reconstruction rows, resulting in values of 3.4 and 3.9 nm for the lower and upper part of the reconstruction rows, respectively. As these values are not integer multiples of the hex unit cell length of 1.4 nm along this direction, this experimental finding indicates the presence of two domains in the hex layer which are displaced with respect to each other. A surface "dislocation" is located between the dotted reconstruction rows running parallel to them. A possible origin of such a dislocation is an antiphasing of coalescing hex domains during the process of the formation of the reconstruction. Figure 2(c) shows the situation of growth stage (2). In contrast to the growth stage (1) in Fig. 2(b), the two reconstruction rows between the dotted hex rows are lifted. The Pt island structure within the hex layer is about 35 nm longer. Again, a bend of the dotted reconstruction rows is found at the end of the Pt island structure (arrow 2). The distance between the dotted hex rows (indicated by the black arrows) has increased to 4.5 nm. The third growth state is imaged in Fig. 2(d) and the change with respect to stage (2) is very similar to the difference between growth states (1) and (2). Again, both hex rows between the dotted reconstruction rows have decayed. Also, the Pt island structure length has increased by about other 32 nm, which is a value very similar to the one found in the former step. At the end of the Pt island structure (arrow 3), two reconstruction rows are found again between the distorted hex rows whose distance is increased by the distortion to about 4.8 nm (black arrows). The inset highlights the well-evolved registry of the Pt islands on the Pt-(1×1) surface. Note the segmented aspect of the elongated Pt island structure, exhibiting right angle breaks in correspondence with the square lattice of the (1×1) surface. Also, note that the segment length approximately coincides with that of the reconstruction unit cell, what seems to indicate that the decay progresses in discrete unit cell jumps. In this way, it may be concluded that the lifting of the reconstruction within the hex layer along a surface "dislocation" line follows a certain periodic behavior, although the details of the surface restructuring mechanism remain unclear.

B. Growth

The morphology of the film in the early stages of growth is well represented in the images of Figs. 3(a)–3(d). Cobalt grows forming islands elongated along the direction of the surface reconstruction columns. This can be seen in the STM images of Figs. 3(a) and 3(b), corresponding to a coverage of $\sim0.20\pm0.05$ ML. The elongated shape is indicative of an anisotropic diffusion of the cobalt atoms as a result of a larger surface mobility in the direction parallel to the reconstruction rows. This may arise from the lower corrugation along the rows than across them (see Fig. 1). Similar evidence of anisotropic diffusion on this surface has also been observed for the growth of Au (Ref. 34) and for the homoepitaxial growth of Pt.[42]

In addition to the anisotropic island shape, Fig. 3(b) clearly shows that these Co islands have very large plateaus and corresponding line profiles (not shown) indicate a monatomic step height. Only a small second layer coverage is present, which appears as brighter regions in the islands. It is interesting to note that the Pt hex reconstruction is preserved in the island surroundings. The picture changes for higher coverage. Figures 3(c) and 3(d) show that for a coverage of ~0.6 ML an intermediate situation is found. The surface reconstruction persists in some regions, while in others the presence of big cobalt islands lifts the reconstruction in their vicinity and produces regions of (1×1) periodicity. From the boundary between the hex and (1×1) surface phases, Fig.

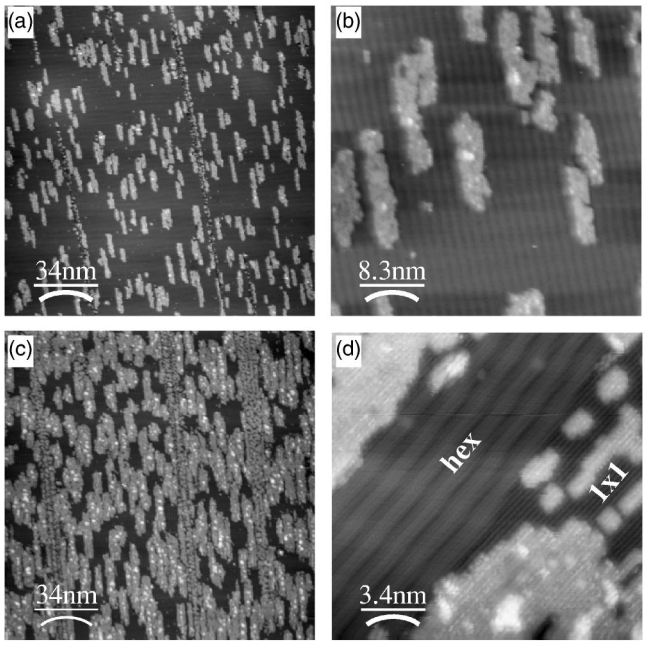

FIG. 3. Morphology at early growth stages of the cobalt layer. Images (a),(b) for ~0.2 ML (V_{gap}=+0.30 V, I=10 and 24 nA); images (c),(d) for ~0.6 ML (V_{gap}=+0.02 and 0.04 V, I=30 and 34 nA).

3(d) it can be seen that the hexagonal reconstruction transits smoothly into the different (1×1) arrangement. The presence of these (1×1) regions suggests that the reconstruction is also removed below the islands. Indeed, careful examination of the STM image of Fig. 3(d) reveals the presence in the Co islands of a line structure that matches the (1×1) period of the unreconstructed substrate. As discussed below, SXRD detects a complete lifting of the reconstruction underneath of 1 ML Co film, and according to the STM image in Fig. 4(a), at 95% of the completion of the first monolayer the second layer coverage is ~5%. An interesting question related to the destabilization of the reconstruction by the Co atoms is where are the excess Pt atoms located in the Co/Pt interface, as the reconstructed layer has 20–25% more atoms than the (1×1). To try to get an answer, a series of topographic line profiles extracted from several images were analyzed to try to distinguish Co and Pt atoms by differences in

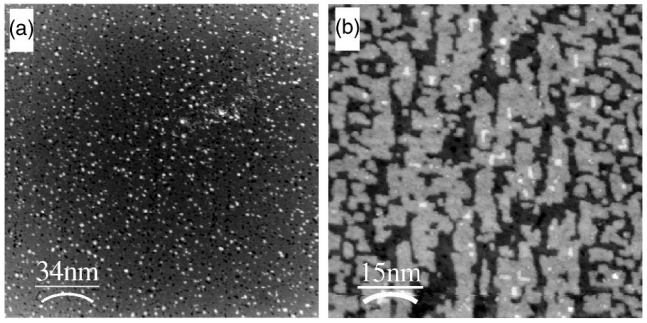

FIG. 4. STM images for a coverage of ~1 ML (a) and ~2.7 ML (b) The growth mode is layer by layer keeping a low roughness. (V_{gap}=−0.03 V, I=20 nA, and V_{gap}=−0.20 V, I=2 nA).

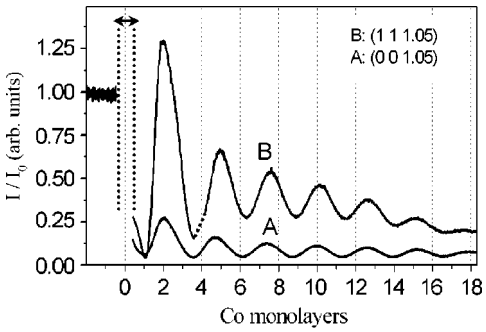

FIG. 5. Evolution of the diffracted x-ray intensity during the deposition of the Co layer. Curve A: specular intensity at (0 0 1.05), probing vertical order; curve B: diffracted intensity at (1 1 1.05), probing both vertical and in-plane order. [Note the short arrow indicating the absence of data during the time required for the manual opening of the evaporator shutter and to perform the experimental x-ray hutch interlock safety routine. The dashed line in curve (1 1 1.05) at about 4 deposited monolayers marks the lack of intensity data due to an x-ray beam failure. The evaporation had to be interrupted and continued about 10 minutes later.]

height. Unfortunately, the data did not allow any clear conclusion. However, visual inspection of images, allows us to give a tentative answer. We observed in several cases small islands surrounded by areas with (1×1) periodicity. Figure 3(d) shows an example in the three small islands at the right side of the image. The area of the (1×1) region is somewhat larger than that of the islands. We argue that all or part of the excess Pt atoms that are "segregated" upon deconstruction of the surface, nucleate in the small islands shown in the figure, as was suggested by the previous study of the lifting of the surface reconstruction in Sec. III A. Further deposition of Co should result in buried Pt islands causing chemical roughness at the interface. One should also consider Co-Pt alloying as another possibility. We did not observe any evidence, based on x-ray diffraction data, on the formation of interface alloys at room temperature exhibiting a unit cell with intermediate parameters to those of Co and Pt. Also, our previous work on x-ray diffraction from Co/Pt(111)[51] and the STM work by Lundgren *et al.*[41,46] on the same system, did not show significant surface alloying for room temperature deposited films. Thus, the hypothesis of clustering appears as a more reasonable answer to the above question. It is worth mentioning that the initial stages of growth described here develop in a similar way to what has been shown for the case of Au on Pt(001)-hex.[34]

Beyond 1 ML, the growth continues in an almost layer-by-layer mode, keeping a low surface roughness, as shown in Fig. 4(b). The estimated Co coverage of the four levels of the deposited layer is as follows: 1st: full, 2nd: 98%, 3rd: 65%, and 4th: 1.5%.

The growth mode of the Co film can also be monitored by measuring during the deposition the temporal evolution of the reflected x-ray intensity at one of the so-called anti-Bragg points or anti-phase conditions in the reciprocal space,[43] as shown in Fig. 5.

The oscillatory behavior is indicative of a layer by layer growth. The rather low values of the intensities during

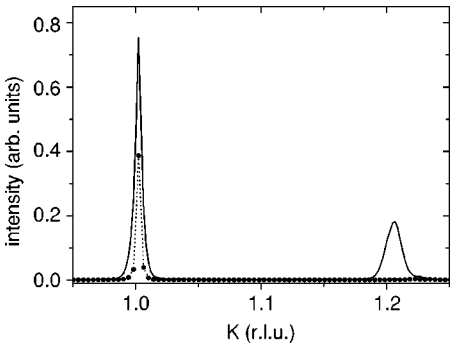

FIG. 6. In-plane x-ray diffraction scans before (continuous line) and after (point line) the evaporation of a 26.1 Å Co film (see the text).

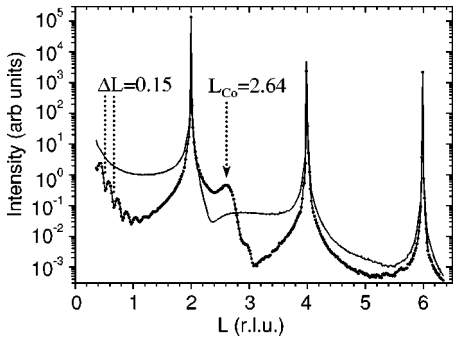

FIG. 7. X-ray extended reflectivity measurements before (continuous line) and after (point line) the evaporation of a 26.1 Å Co film. Note the Pt bulk Bragg peaks at integer L values, the Co peak at $L=2.64$ and the Kiessig fringes at low L values arising from the interference between scattering by the two interfaces of the Co layer.

growth are due to imperfections in the ideal growth. However, it is not straightforward to infer the surface roughness directly from the attenuation of the intensities, since the reconstruction of the starting surface before the deposition complicates somewhat the analysis compared to the case of the growth on an unreconstructed surfaces as in Co/Pt(111).[51] As the reconstructed surface contains 20–25% excess Pt atoms in a hexagonal arrangement that does not match the underlying square lattice, the specular rod, before the deposition starts, has more Pt atoms contributing to the intensity than the (11 L) rod since in the latter the hexagonal topmost plane does not contribute. When Co is deposited, the underlying Pt atoms evolve from the hexagonal layer to the unreconstructed 1×1 surface. This results in an extra intensity, since, in addition to the change in intensity due to the deposited Co, there is another change due to the Pt atoms that become in register with the (001) lattice. Taking into account this fact, a numerical simulation assuming that after deposition of one Co layer the Pt surface is fully reconstructed, reproduce the observed results in the figure: namely that the maximum at 2 deposited layers is more intense for (111) than for the (001) and that the overall intensity of the (111) peak is more intense (relative to the initial intensity prior to deposition) than the (001). It is important to note that the observation of several clear growth oscillations in the curves proves that the Co layers present vertical and in-plane order. Indeed, the close similarity between both curves is a strong evidence of pseudomorphic growth.

C. Structure of the cobalt film

As evidenced by STM (see Figs. 3 and 4) and XRD (not shown), one monolayer of Co suffices to remove the Pt surface reconstruction. As the misfit between the fcc Co and Pt lattices is very large ($\sim10\%$) one would expect, as is the case for Co/Pt(111),[44–46] a relaxed fcc Co layer on top of the Pt substrate giving rise to a coincidence lattice of periodicity close to 10 times the substrate periodicity. Surprisingly, this does not occur for Co/Pt(001). Figure 6 shows the in-plane (0 K 0.15) scans before and after the Co deposition. For the clean surface, two peaks are noticeable: a first peak at $K=1.0$ arises from the (01L) Pt crystal truncation rod, and a second one at $K=1.21$ is characteristic of the reconstructed surface layer.[33] After deposition of a 17.5 ML Co film, the peak intensity at $K=1.21$ is reduced by a factor of $\simeq100$ and that of the peak at $K=1.0$ by only a factor of $\simeq2$. The large attenuation of the peak at $K=1.21$ indicates that the Pt(001)-hex reconstruction is widely lifted, while the attenuation of the $K=1.0$ peak can be explained by the interference between the scattering of the Co and Pt layers. The narrowing of the $K=1.0$ peak indicates an increase of the lateral size of the surface 1×1 domains. If the Co layer were fully relaxed, one should find an intense peak at $K=1.09$ [as was found previously for Co/Pt(111); see Fig. 5 in Ref. 51]. Note that this in-plane peak of a relaxed Co layer is not found (Fig. 6).

The absence of a peak at (0 1.09 0.15) could be due to several reasons: (a) the overlayer is disordered in the surface plane, (b) there is a rotational epitaxy that produces reflections away from the crystallographic surface directions, (c) the Co film is pseudomorphic with the Pt(001)-(1×1) substrate. The first possibility is unlikely in view of the nice oscillatory evolution of the diffracted intensity at (1 1 1.05), as depicted in Fig. 5(b); the second possibility was thoroughly explored without success; thus, we concluded that the growth is pseudomorphic.

The study of the vertical order of the Co layer also gives a strong indication of pseudomorphic growth. The vertical order was probed by the measurement of the specular reflectivity extended through several Brillouin zones, as shown in Fig. 7. The small ripples visible at $0.2\leqslant L\leqslant1.2$, the so-called Kiessig fringes, have a period of $\Delta L=0.15\pm0.01$, from which a thickness of the Co film of $3.923\ \text{Å}/0.15=26.1(\pm2.0\ \text{Å})$ is deduced. This thickness determination is more precise than that made by counting oscillations of the reflected intensity in an antiphase condition, but both methods produce consistent results for the thickness within 15–20% accuracy. The sharp peaks at integer L values are the bulk Bragg reflections of the Pt crystal, and the peak at $L=2.64\pm0.01$ arises from diffraction of the stack of Co planes. From the position of the cobalt peak, $L=2.64$, a value of 1.485 ± 0.005 Å for the vertical interplanar distance in the Co layer is directly obtained, and which is taken as the corresponding thickness per Co monolayer. This value is very different from the interplanar distance between fcc Co (100)

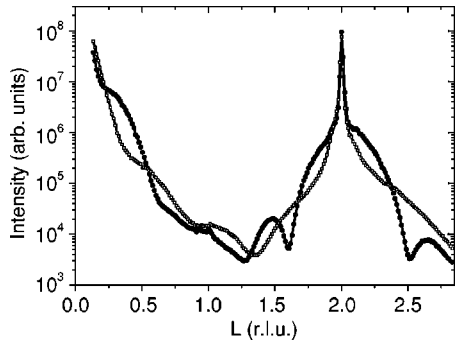

FIG. 8. X-ray specular reflectivity. Unfilled squares: Co(5.9 Å)/Pt(001); filled circles: Pt(3.3 Å)/Co(5.9 Å)/Pt(001).

planes, 1.772 Å, or fcc or hcp Co (111) planes, 2.046 Å.[47] However, it is very close to that of bcc Co (001) planes, 1.41(3) Å.[48] In addition, a bcc Co lattice with (001) orientation and 2.82(6) Å lattice size matches the in-plane symmetry and fits well the 2.774 Å in-plane lattice of the Pt substrate. These observations suggest that the structure of the Co film is close to bcc. The in-plane pseudomorphism would imply a compressive strain in the Co film of **(**2.774 −2.82(5)**)**/2.82(5)=−1.8%, while out of the surface plane, the strain is tensile, (1.485−1.41(3))/1.41(3)=5.1%. It is noticeable that this yields a unit cell volume only differing from that of the bcc by 1.4%. Therefore, we conclude that the Co film has a body centered cubic cell with a tetragonal distortion of $c/a=(2*1.485)/2.774=1.071$, i.e. of 7%, and a volume change of 1.4%, which is pseudomorphic to the Pt(001)-(1×1) surface. This structure has been found to be stable for thickness up to at least ~20 ML. Note that Co fcc lattice can be seen as a bct with $c/a=3.544/2.506=1.41$, while a bcc has $c/a=1.0$; thus, our bct structure is very much closer to bcc than fcc. Indeed, the surface diffraction rods of a pseudomorphic bcc Co layer strictly coincide with the crystal truncation rods of the Pt bct substrate, with the only difference of the positions in L of the peaks related to their different vertical interplanar distances.

Beside this findings, XRD and STM data presented some additional features that suggest a partial relaxation of the in-plane compressive strain. A detailed description will be reported in a further publication.[49]

D. Growth of bcc-Co/fcc-Pt(001) superlattices

We examined the possibility of growing epitaxial Co/Pt 001-oriented superlattices in different experiments. Figure 8 shows the specular reflectivity measurements on an epitaxial Pt(3.3 Å)/Co(5.9 Å)/Pt(001) trilayer. For all the growth steps, oscillations of the specular intensity similar to those in Fig. 5 were observed. The (0 0 L) scans in Fig. 8 show clear Kiessig fringes, which is an indication of film perfection and low roughness. No sign of relaxation was found in the in-plane scans. This is considered as evidence for the pseudomorphism, as in the previously discussed case of single Co films on Pt(001).

IV. MAGNETIC PROPERTIES

In Co/Pt ultrathin films the magnetic properties are determined not only by the ferromagnetic cobalt layer but also by the interface via the induced magnetism of the platinum. The combination of TMOKE and magnetic-resonant SXRD at the Pt L_{III} absorption edge allows us to probe independently the magnetism of either the cobalt film or that of the interface platinum atoms, respectively.

Figures 9(a) and 9(b) show magnetization cycles measured by magnetic-resonant SXRD detected at $(HKL)=(0\ 2\ 2.44)$ in the reciprocal space and by TMOKE, respectively, for a 6.9 Å Co film. Both cycles represent the in-plane magnetization and their shape evidences the presence of in-

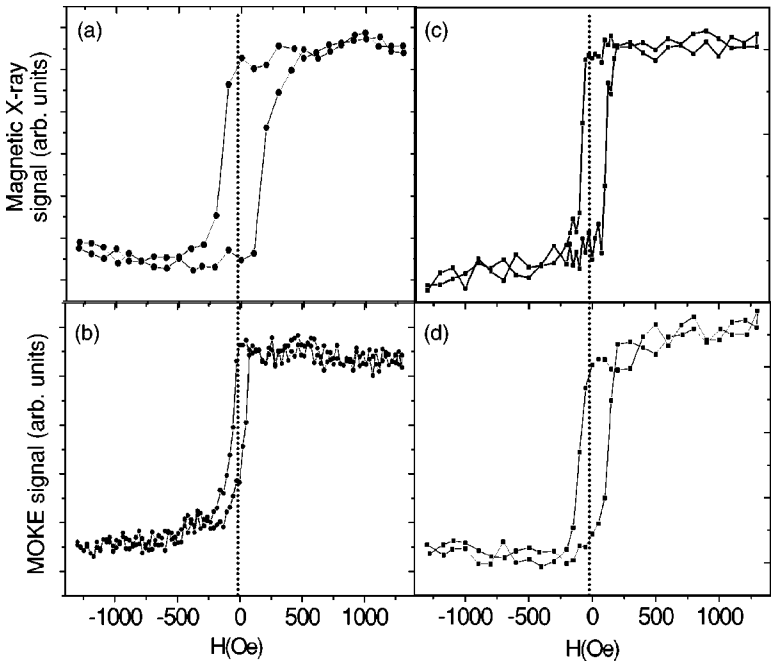

FIG. 9. Magnetic hysteresis loops for Pt [panels (a), (c)] and Co [panels (b), (d)] measured by magnetic-resonant SXRD and TMOKE techniques, respectively. Loops (a), (b) are for a Co(6.9 Å)/Pt(001) film; loops (c), (d) for a Pt(2.2 Å)/Co(6.9 Å)/Pt(001) film.

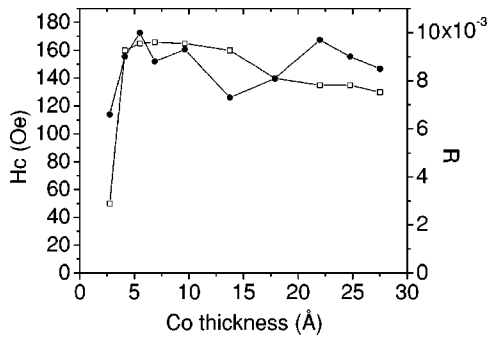

FIG. 10. Dependence on the Co layer thickness of the coercive force, *Hc* (unfilled squares) and the asymmetry ratio, *R* (filled circles) of the Pt x-ray loops measured at $(H\ K\ L)=(0\ 0\ 2.44)$.

plane easy axes of magnetic anisotropy. The coercitivities are however different: that of the Pt interface (a) is clearly larger than that of the TMOKE cycle (b). This difference seems to suggest that at the interface the Co/Pt system is magnetically harder. Nevertheless, further investigation is needed to clarify this point. Panels (c) and (d) show magnetization loops from a Pt(2.2 Å)/Co(6.9 Å)/Pt(001) trilayer as measured with x rays and TMOKE, respectively. Again the cycles evidence in-plane easy axes of magnetic anisotropy. In this case the coercive forces found in the Pt and Co loops are similar.

Figure 10 depicts the dependence on the Co layer thickness of the asymmetry ratio, *R*, and the coercive force, *Hc*, of the Pt x ray loops. At the lowest thickness investigated (1.4 Å) no magnetic signals are detectable. At 2.7 Å the cycle (not shown) presents very small remanence and low coercitivity, resembling that of a superparamagnet. At 4.1 Å the shape of the hysteresis loop is already rectangular and the Pt magnetic signal reaches a value which does not change significantly upon further Co deposition. As shown in Fig. 10, the coercive field reaches a maximum plateau of ~165 Oe at a thickness of 5–10 Å and for thicker films decreases continuously down to 140 Oe at ~26 Å. We have investigated if this decrease could be due to contamination effects from the residual gas. We have found that, on the contrary, oxygen contamination tends to increase the coercitivity. The decrease of coercive fields may be related to the diminishing effect of the interface for a thicker Co film.

The relative change in the diffraction signal due to magnetic scattering at (0,0,2.44) is approximately $R\sim 1\%$ (Fig. 10). These values are comparable to those found in previous work[50,51] for Co films deposited at low temperature on Pt(111). This indicates, as an estimate, that the induced magnetic moment of Pt is similar in both cases, thus of the order of $0.2\mu_B$. Nevertheless, in order to give a precise value of the Pt magnetic moment measurements and a detailed analysis of the magnetic Pt crystal truncation rods are required. Moreover, the possible presence of a certain amount of excess Pt atoms mixed in the first Co layer and with a large induced magnetic moment complicates the analysis. If the Pt magnetic moments are no longer confined in a single interfacial atomic plane, the interference between the magnetic scattering signals arising from the magnetic Pt atoms in different interfacial layers need to be also taken into account.

V. DISCUSSION AND CONCLUDING REMARKS

To summarize, we have found that Co grows on Pt(001) in a layer-by-layer mode up to the investigated thickness (~30 Å). The crystalline structure of the Co films is a tetragonally distorted bcc in pseudomorphic epitaxy with the substrate. The distortion consists of a −1.8% compressive strain in the plane and a tensile strain of 5.1% out of plane.

Similar stabilization of bcc or bct cobalt phases in ultrathin films like the one reported in this work has already been observed for a variety of substrates, such as GaAs(110),[48] Fe(001),[52] Cr(100),[53] FeAl(001),[54] W(100),[55] Pd(001),[23] Cr(110),[56] and Au(001).[57]

The bct Co films exhibit in-plane easy axes of magnetic anisotropy within the thickness range of 5–30 Å. The magnetization curves of the Co layer and the interfacial Pt are similar, indicating ferromagnetic coupling.

Let us compare our results with previously published work. In-plane anisotropy in Co/Pt superlattices with (001) orientation was reported by Lee *et al.*[12–16] for the Co layer thickness above 1 ML. The structure of the Co film was considered to be distorted fcc. Boeglin *et al.* reported structural results from LEED on Co/Pt(001).[19–21] Above 1.5 ML of Co, they observed that LEED patterns became fuzzy and interpreted this as being due to a disordered film. Pütter *et al.*[22] based on LEED/MEED observations concluded a layer-by-layer growth of the Co layer, which is pseudomorphic up to 1 ML and relaxed at higher coverage.

Engel *et al.*[24,25] investigated Co/Pd(001), which is closely related to Co/Pt(001) since the lattice parameters of Pd and Pt differ by less than 1%. They observed a pseudomorphic epitaxy. More recently Giordano *et al.*[23,26] found in the same system by LEED and photoelectron diffraction a bct structure, stable up to ~30 ML. Interestingly, Co/Pd(001) also displays in-plane magnetic anisotropy. It was concluded that the strain of the pseudomorphic Co layer gives rise to a magnetostriction contribution that adds to the shape anisotropy to favor in-plane magnetic anisotropy and accounts for the large volume anisotropies measured.[10,25] The same argumentation should remain valid for our case, in view of the close structural similarities. Note that the magnetocrystalline anisotropy is expected to be very small since the unit cell is almost cubic and has (001) orientation, causing the equivalence of the in-plane and out-of-plane directions corresponding to the crystal axes.

ACKNOWLEDGMENTS

The authors acknowledge the technical help of H. Isern, E. Paiser, L. Petit, V. A. Solé, K. Larsson, and P. Bencok. The use of the software WSxM©; http://www.nanotec.es is also acknowledged.

*Corresponding author. Electronic address: valvidares@esrf.fr

[1] Magnetism in the Nineties (special issue), J. Magn. Magn. Mater. **100** (1991).
[2] Magnetism beyond 2000 (special issue), J. Magn. Magn. Mater. **200** (1999).
[3] J. B. Kortright, D. D. Awschalom, J. Stohr, S. D. Bader, Y. U. Idzerda, S. S. P. Parkin, I. K. Schuller, and H. C. Siegmann, J. Magn. Magn. Mater. **207**, 7 (1999).
[4] S. D. Bader, Surf. Sci. **500**, 172 (2002).
[5] J. Shen and J. Kirschner, Surf. Sci. **500**, 300 (2002).
[6] P. F. Carcia, J. Appl. Phys. **63**, 5066 (1988).
[7] F. J. A. den Broeder, H. C. Donkersloot, H. J. G. Draaisma, and W. J. M. de Jonge, J. Appl. Phys. **61**, 4317 (1987).
[8] L. Néel, J. Phys. Radium **15**, 225 (1954).
[9] U. Gradmann and J. Müller, Phys. Status Solidi **27**, 313 (1968).
[10] M. T. Johnson, P. J. H. Bloemen, F. J. A. den Broeder, and J. J. de Vries, Rep. Prog. Phys. **59**, 1409 (1996).
[11] M. Farle, Rep. Prog. Phys. **61**, 755 (1998).
[12] C. H. Lee, R. F. C. Farrow, C. J. Lin, E. E. Marinero, and C. J. Chien, Phys. Rev. B **42**, 11 384 (1990).
[13] C. H. Lee, R. F. C. Farrow, B. D. Hermsmeier, R. F. Marks, W. R. Bennett, C. J. Lin, E. Marinero, P. D. Kirchner, and C. J. Chien, J. Magn. Magn. Mater. **93**, 592 (1991).
[14] C. J. Chien, R. F. C. Farrow, C. H. Lee, C. J. Lin, and E. E. Marinero, J. Magn. Magn. Mater. **91**, 47 (1991).
[15] C. J. Lin, G. L. Gorman, C. H. Lee, R. F. C. Farrow, E. E. Marinero, H. V. Do, H. Notarys, and C. J. Chien, J. Magn. Magn. Mater. **93**, 194 (1991).
[16] B. D. Hermsmeier, R. F. C. Farrow, C. H. Lee, E. Marinero, C. J. Lin, R. F. Marks, and C. J. Chien, J. Appl. Phys. **69**, 5647 (1991).
[17] J. V. Harzer, B. Hillebrands, R. L. Stamps, G. Güntherodt, D. Weller, C. H. Lee, R. F. C. Farrow, and E. E. Marinero, J. Magn. Magn. Mater. **92**, 104 (1992).
[18] B. Zhang, K. M. Krishnan, C. H. Lee, and R. F. C. Farrow, J. Appl. Phys. **73**, 6198 (1993).
[19] C. Boeglin, A. Barbier, B. Carrière, R. Cousandier, J. P. Deville, F. Scheurer, and C. Speisser, Surf. Sci. **251/252**, 602 (1991).
[20] C. Boeglin, A. Barbier, F. Scheurer, B. Carrière, and J. P. Deville, J. Magn. Magn. Mater. **93**, 31 (1991).
[21] C. Boeglin, B. Carrière, J. P. Deville, F. Scheurer, C. Guillot, and N. Barrett, Phys. Rev. B **45**, 3834 (1992).
[22] S. Pütter, J. Hoyer, and H. P. Oepen, in *XVIII Int. Coloq. Mag. Films and Surf.*, 2003.
[23] H. Giordano, A. Atrei, M. Torrini, U. Bardi, M. Gleeson, and C. Barnes, Phys. Rev. B **54**, 11 762 (1996).
[24] B. N. Engel, C. D. England, R. A. VanLeeuwen, M. H. Wiedmann, and C. M. Falco, Phys. Rev. Lett. **67**, 1910 (1991).
[25] B. N. Engel, C. D. England, R. A. V. Leewen, M. H. Wiedmann, and C. M. Falco, J. Appl. Phys. **70**, 5873 (1991).
[26] H. Giordano, A. Atrei, G. Rovida, M. Torrini, and U. Bardi, J. Electron Spectrosc. Relat. Phenom. **76**, 455 (1995).
[27] S. Ferrer and F. Comin, Rev. Sci. Instrum. **66**, 1674 (1995).
[28] S. Ferrer, P. Fajardo, F. de Bergevin, J. Alvarez, X. Torrelles, H. A. van der Vegt, and V. H. Etgens, Phys. Rev. Lett. **77**, 747 (1996).
[29] S. Hagstrom, H. B. Lyon, and G. A. Samorjai, Phys. Rev. Lett. **15**, 491 (1965).
[30] M. V. Hove, R. J. Koestner, P. C. Stair, J. P. Bibérian, L. L. Kesmodel, I. Bartoš, and G. A. Somorjai, Surf. Sci. **103**, 189 (1981).
[31] K. Kuhnke, K. Kern, G. Comsa, and W. Moritz, Phys. Rev. B **45**, 14 388 (1992).
[32] D. L. Abernathy, S. G. J. Mochrie, D. M. Zehner, G. Grübel, and D. Gibbs, Phys. Rev. B **45**, 9272 (1992).
[33] G. Ritz, M. Schmid, P. Varga, A. Borg, and M. Rønning, Phys. Rev. B **56**, 10 518 (1997).
[34] C. Berg, H. J. Venvik, F. Strisland, A. Ramstad, and A. Borg, Surf. Sci. **409**, 1 (1998).
[35] V. Fiorentini, M. Methfessel, and M. Scheffler, Phys. Rev. Lett. **71**, 1051 (1993).
[36] P. van Beurden, B. S. Bunnik, G. J. Kramer, and A. Borg, Phys. Rev. Lett. **90**, 066106 (2003).
[37] R. J. Behm, P. A. Thiel, P. R. Norton, and G. Ertl, J. Chem. Phys. **78**, 7437 (1983).
[38] P. A. Thiel, R. J. Behm, P. R. Norton, and G. Ertl, J. Chem. Phys. **78**, 7448 (1983).
[39] R. J. Behm, in *Diffusion at Interfaces: Microscopic Concepts* (Springer-Verlag, Berlin, 1987), Chap. on Topography Modification and Microscopic Motion on Metal Surfaces.
[40] I. V. Markov, *Crystal Growth for Beginners: Fundamentals of Nucleation, Crystal Growth and Epitaxy* (World Scientific, Singapore, 1995).
[41] E. Lundgren, B. Stanka, W. Koprolin, M. Schmid, and P. Varga, Surf. Sci. **423**, 357 (1999).
[42] T. R. Linderoth, J. J. Mortensen, K. W. Jacobsen, E. Laegsgaard, I. Stensgaard, and F. Besenbacher, Phys. Rev. Lett. **77**, 87 (1996).
[43] I. K. Robinson and D. J. Tweet, Rep. Prog. Phys. **55**, 599 (1992).
[44] P. Grutter and U. T. Durig, Phys. Rev. B **49**, 2021 (1994).
[45] S. Ferrer, J. Alvarez, E. Lundgren, X. Torrelles, P. Fajardo, and F. Boscherini, Phys. Rev. B **56**, 9848 (1997).
[46] E. Lundgren, B. Stanka, M. Schmid, and P. Varga, Phys. Rev. B **62**, 2843 (2000).
[47] *Landolt-Börnstein, New Series III/19a* (Springer-Verlag, Berlin).
[48] G. A. Prinz, Phys. Rev. Lett. **54**, 1051 (1985).
[49] S. Ferrer *et al.*, in preparation.
[50] S. Ferrer, J. Alvarez, X. Torrelles, E. Lundgren, and P. Fajardo, Physica B **248**, 9 (1998).
[51] O. Robach, C. Quiròs, P. Steadman, K. F. Peters, E. Lundgren, J. Alvarez, H. Isern, and S. Ferrer, Phys. Rev. B **65**, 054423 (2002).
[52] H. Li and B. P. Tonner, Phys. Rev. B **40**, 10 241 (1989).
[53] F. Scheurer, B. Carrière, J. P. Deville, and E. Beaurepaire, Surf. Sci. Lett. **245**, L175 (1991).
[54] C. P. Wang, S. C. Wu, F. Jona, and P. M. Marcus, Phys. Rev. B **49**, 17 385 (1994).
[55] H. Wormeester, E. Hüger, and E. Bauer, Phys. Rev. Lett. **77**, 1540 (1996).
[56] S. Fölsch, A. Helms, A. Steidinger, and K. H. Rieder, J. Magn. Magn. Mater. **191**, 38 (1999).
[57] N. Sapiridis, T. Ślęzak, and J. Korecki, in *Proceedings of the 22th ECOSS Conference*, to appear in Surf. Sci. (2003).